

Received 14 April 2021; revised 11 June 2021; accepted 5 July 2021. Date of publication 8 July 2021; date of current version 15 July 2021.  
The review of this article was arranged by Editor C. Surya.

Digital Object Identifier 10.1109/JEDS.2021.3095501

# Two-Dimensional Transient Temperature Distribution Measurement of GaN Light-Emitting Diode Using High Speed Camera

GUANGHENG XIAO, WUJUN DU, ZHIYUN WANG, GUOLONG CHEN, LIHONG ZHU<sup>1</sup>, YULIN GAO<sup>1</sup>,  
ZHONG CHEN<sup>1</sup>, ZIQUAN GUO (Member, IEEE), AND YIJUN LU<sup>1</sup>

Department of Electronic Science, Fujian Engineering Research Center for Solid-State Lighting, Xiamen University, Xiamen 361005, China

CORRESPONDING AUTHORS: Z. GUO AND Y. LU (e-mail: zqguo@xmu.edu.cn; yjlu@xmu.edu.cn)

This work was supported in part by the National Natural Science Foundation of China under Grant 51802083; in part by the Major Science and Technology Project of Fujian Province under Grant 2018H6022 and Grant 2019H6004; and in part by the Natural Science Foundation of Fujian Province under Grant 2019J05022.

(Guangheng Xiao and Wujun Du contributed equally to this work.)

**ABSTRACT** We put forward a non-contact method for determining the transient two-dimensional (2D) temperature distribution of light emitting diodes (LEDs). A high-speed camera is employed to acquire the 2D reflective light of blue LED under test (468 nm) illuminated by a red LED (690 nm) as the incident light source to avoid the band-gap modulation effect. The 2D transient temperature distribution is derived in terms of temperature-dependent reflective light intensity relationship. Two cases are studied to test the system in this work under (1) 1980 fps frame rate with time resolution of 505  $\mu$ s at 300 mA, and (2) 5600 fps with time resolution of 179  $\mu$ s at 500 mA. Compared with the conventional infrared thermal imaging (TI) method, the spatial resolution and the time resolution of this proposed method increase up to one and two orders of magnitude, respectively.

**INDEX TERMS** GaN LED, reflective light, transient temperature, high speed camera.

## I. INTRODUCTION

The GaN-based light emitting diodes (LEDs) have been widely applied in the lighting and display fields, including the general lighting and micro- or mini-LED displays [1]. The P-N junction temperature of GaN LED is a key parameter for evaluating the performance of GaN-based LED. The rise of junction temperature in devices would not only lower the luminous efficiency [2], but also decrease the lifetime of LEDs [3]. Therefore, the junction temperature test is of significance for semiconductor devices.

Currently, there are numbers of methods for detecting junction temperature in GaN-based LED. The micro-thermocouple method ( $\mu$ -TC), a conventional direct contact method for measuring the naked surface temperature of semiconductor device, fails to touch the chip surface of encapsulated device. As a non-contact method, the thermal imaging (TI) camera can be used to detect the two-dimensional (2D) naked surface temperature of semiconductor device, but the spatial resolution is not

eligible for micro-size device [4]. Besides, the time resolution of the TI method is not fast enough either. The emissivity in the TI measurement is also hard to be accurately determined for various materials in GaN LED, such as the cathodes and anodes. Other reported methods like the forward voltage [5], [6], centroid wavelength [7], peak wavelength [8], full width at half maximum [9], normalized emission power [10], blue-white ratio [11], Raman spectroscopy [12], [13], bi-directional thermal resistance [14], Micro-infrared Imaging [15], etc., are generally adopted to measure the average junction temperature of GaN-based LED. Recently, our research group has carried out several studies about measuring 2D surface temperature of GaN LED based on the hyperspectral imaging technology [7], [16].

In this work, we put forward a non-contact method combining the high-speed camera and the reflective light intensity method (referred to as h-SCRLI hereafter) to detect the transient 2D temperature of LED under test (LUT). This solution owns merits of both high spatial resolution at submicron

scale and high time resolution at the level of 100  $\mu\text{s}$ , and is useful for the dynamic thermal detection of LED chips.

## II. THEORY OF H-SCRLI METHOD

The h-SCRLI method is based on the principle of linear temperature dependent surface reflectivity of GaN LED. Thus, we can use the high-speed camera to capture the reflected photons and derive 2D temperature distribution in terms of light intensity change. The relationship of the reflectivity of GaN LED and the temperature can be written as [10],

$$R(T) = R(T_0) + \frac{dR}{dT}(T - T_0) \quad (1)$$

where  $R(T)$  represents the surface reflectivity at temperature  $T$ . Experimentally, the  $R(T)$  can be replaced by reflected light intensity. Hence, the above equation can be re-written as,

$$T_s = T_0 + K_L[L(T_s) - L(T_0)] = T_0 + K_L \Delta L \quad (2)$$

where  $T_s$  is the surface temperature of GaN LED,  $K_L$  is the temperature sensitive parameter (TSP),  $L(T_s)$  and  $L(T_0)$  are the reflected light intensity at the temperature of  $T_s$  and  $T_0$ , respectively, and  $\Delta L$  is the relative variance of reflected light intensity.

Prior to calculating the transient 2D temperature distribution of the LUT, pre-processing the 2D reflected light intensity image acquired by the camera is required, including rotation and alignment of image, chip profile extraction from the whole image. Therefore, the sub-pixel Shi-Tomasi corner detection algorithm is employed to locate the LED chip profile. The formula for calculating the final response value of the corner point of  $R$  is shown as:

$$R = \min(\lambda_1, \lambda_2) \quad (3)$$

where  $\lambda_1$  and  $\lambda_2$  represent the eigenvalues of the gradient matrix. The core of this algorithm is to use the local window  $h(m,n)$  to move on the image to determine where the gray level changes significantly. The corner point is determined when the gray level of the window changes significantly in all directions. During the experiment, the orientation of LED chip may be changed. Therefore, the bilinear difference method and the backward mapping method are both used to rotate and align the image so that the LED profile can be accurately and conveniently extracted.

## III. EXPERIMENTAL SETUP AND PROCEDURE

The experimental system for measuring the dynamic two-dimensional temperature distribution of LEDs is shown in Fig. 1(a). The measurement setup mainly contains high speed camera (2) (HK-A1281-CC500/CM500), microscope with a high-pass filter (3), blue LUT (5), incident red LED (7), Heat sink (6) with temperature controller (8) (9) (Whtalent TEC, SourceMeter 2510), electrical source meter (10) (11) (KeySight 2912, Yokogawa GS610) for blue LUT and incident red LED, respectively.

The bare blue LED (468 nm) with 1 mm $\times$ 1 mm chip size is used as the LED under test. The reason of selecting

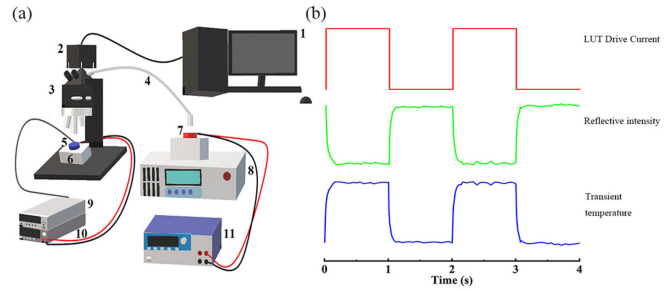


**FIGURE 1. (a) The experimental system for measuring the dynamic two-dimensional temperature distribution. (b) Illustration of drive current waveform of LUT, acquisition waveform of camera and processed transient temperature waveform.**

bare chip attributes to the convenient comparison with the TI method. During the calibration of coefficient matrix, the heat sink of LUT is adjusted from 25  $^{\circ}\text{C}$  to 50  $^{\circ}\text{C}$  with an increment of 5  $^{\circ}\text{C}$ . During the measurement, the LUT is driven with square wave current of 2 s period and amplitude of 300 mA or 500 mA by an electrical source meter (KeySight 2912).

The 690 nm red LED with temperature stabilized at 25 $^{\circ}\text{C}$  and power supplied at 800 mA by an electrical source meter (Yokogawa GS610) provides stable incident light to illuminate LUT. The principle of using red incident light lies in its lower band-gap energy than that of LUT so that the spectral band-gap modulation and unnecessary excitation of LUT by incident light can be avoided. We employ a high-pass filter with a centroid wavelength of about 650 nm to eliminate the light crosstalk from the blue LUT.

Fig. 1(b) depicts the trend of the reflective intensity acquired by high-speed camera and the transient temperature of the LUT in terms of periodic drive current. We apply a high-speed camera to acquire the transient 2D reflective intensity distribution, then, according to the negative linear relationship of the reflective intensity with temperature, perform a series of above-mentioned pre-processing algorithms to obtain the corresponding transient 2D thermal characteristics, especially those at the rising edge and the falling edge, i.e., the heating and cooling process.

Two cases are studied to test the system in this work. Case I: The LUT is driven by 300 mA square wave, the camera runs under 1980 fps frame rate with time resolution of 505  $\mu\text{s}$  and 528 $\times$ 512 pixels in picture size. Case II: The LUT is driven at 500 mA, the camera runs under higher frame rate of 5600 fps with better time resolution of 179  $\mu\text{s}$  and 288 $\times$ 256 pixels in picture size.

## IV. ANALYSES AND DISCUSSIONS

### A. RESULTS OF CASE I

The blue LUT is driven by 300 mA square wave, transient 2D temperature images are taken by the high-speed camera at frame rate of 1980 fps, with about 505  $\mu\text{s}$  time resolution.

Fig. 2 shows a series of transient 2D temperature distribution of the LUT by the h-SCRLI method at the rising edge of drive current, and transient response comparison between

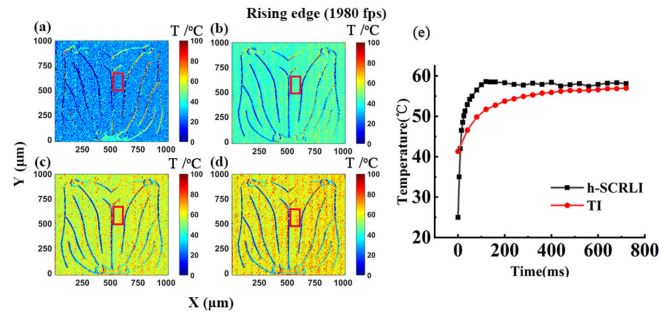


**FIGURE 2.** Transient 2D temperature distribution of the blue LUT driven with 300 mA at the rising edge of (a) 0 ms, (b) 75 ms, (c) 95 ms, and (d) 125 ms. (e) transient response comparison between the proposed method and the TI method.

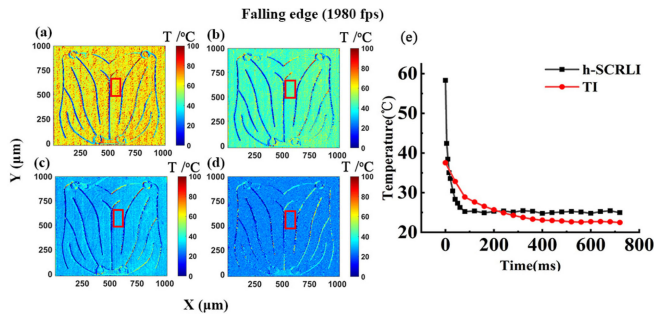


**FIGURE 3.** Transient 2D temperature distribution of the blue LUT driven with 300 mA at the falling edge of (a) 0 ms, (b) 5 ms, (c) 10 ms, (d) 145 ms. (e) transient response comparison between the proposed method and the TI method.

the proposed method and the TI method. The electrodes can be clearly distinguished from the other zones due to their obvious temperature differences. The relative low TSP of electrodes (K coefficient) suggests insensitive temperature response of electrodes to reflective light. Besides, the relative low  $R^2$  indicates higher fitting errors of electrodes temperature compared to the other zones. In general, the temperature trend measured by both methods are basically in agreement, but h-SCRLI method owns better temporal resolution. Under  $528 \times 512$  pixels, the temperature distribution is relatively uniform. On the chip surface, average transient temperature distribution from a  $30 \times 70$  pixels box is extracted to compare with that by TI method, as shown in Fig. 2(e). Notice that the curve measured by h-SCRLI method is much steeper than that by TI, suggesting a faster time response. At the falling edge, as shown in Fig. 3(e), similar phenomenon is found that curve measured by h-SCRLI method decays faster than that by TI. In addition, judging from the curves by h-SCRLI method, it takes about 140 ms at the rising edge (heating process) to reach steady state, while it takes about 80 ms at the falling edge (cooling process) to reach steady state. The phenomenon that the cooling process is faster than the heating process can also be confirmed from corresponding curves by TI.

Fig. 4 demonstrates spatial resolution comparison between the proposed h-SCRLI and the TI method. A horizontal line labeled as L01 is drawn horizontally along chip surface, as

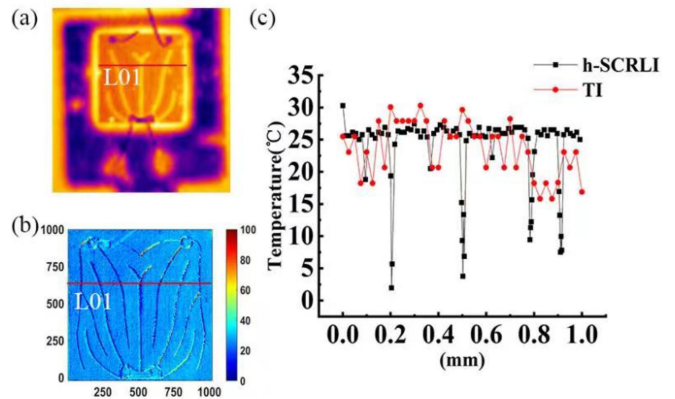


**FIGURE 4.** Spatial resolution comparison between the proposed method and the TI method for Case I. (a) thermal imaging taken by TI, (b) 2D temperature distribution by h-SCRLI, (c) comparison of temperature distribution along L01 between the proposed method and the TI method.

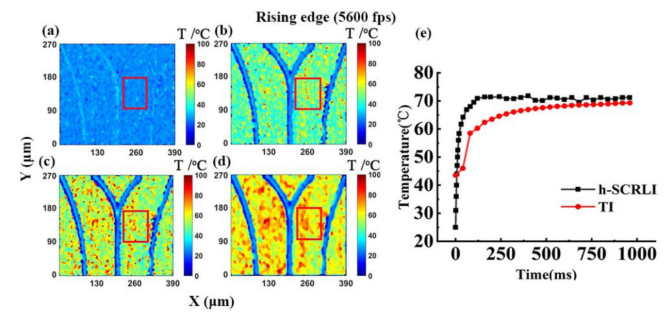


**FIGURE 5.** Transient 2D temperature distribution of the blue LUT driven with 500 mA at the rising edge of (a) 0 ms, (b) 10.8 ms, (c) 23.4 ms, (d) 151.2 ms. (e) time response comparison between the proposed method and the TI method.

displayed in Fig. 4(a) and (b). Fig. 4(c) shows comparison of temperature distribution along L01 between the proposed method and the TI method. The former exhibits much better spatial resolution and sensitivity, and provides more detailed information, especially at the electrodes that is unable to be detected by TI is clearly resolvable by h-SCRLI. The relatively much lower temperature of electrodes is possibly attributed to the low temperature sensitivity of electrodes that results in more fluctuations of temperature fitting. The spatial resolution by h-SCRLI is limited to that of optical microscope, submicron in this system, being estimated by the Rayleigh criterion  $d = 0.61\lambda/NA$ , where  $d$  is the minimum distance between resolvable points,  $\lambda$  is the wavelength of light, 690nm in this case,  $NA$  is the numerical aperture. For a  $10\times$  objective lens with  $NA = 0.28$ ,  $d = 1.5\mu\text{m}$ . For a  $100\times$  objective lens with  $NA = 0.55$ ,  $d = 0.76\mu\text{m}$ .

## B. RESULTS OF CASE II

At 5600 fps, due to the hardware property of the high-speed camera, the picture size shrinks to  $288 \times 256$  pixels, covering only part of the chip size, as shown in Fig. 5 and Fig. 6. In addition, the increase of frame rate leads to less exposure time ( $179 \mu\text{s}$ ).

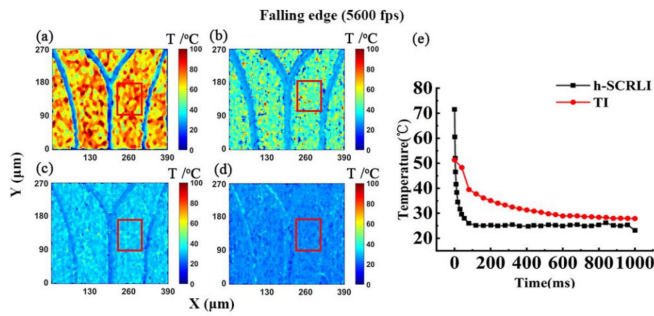


**FIGURE 6.** Transient 2D temperature distribution of the blue LUT driven with 500 mA at the falling edge of (a) 0 ms, (b) 5.4 ms, (c) 55.8 ms, (d) 90 ms. (e) time response comparison between the proposed method and the TI method.

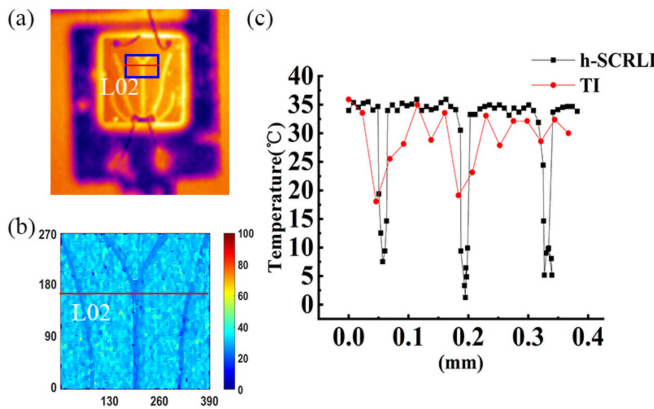


**FIGURE 7.** Spatial resolution comparison between the proposed method and the TI method for Case II. (a) thermal imaging taken by TI, (b) 2D temperature distribution by h-SCRLI, (c) comparison of temperature distribution along L02 between the proposed method and the TI method.

Thus, more additional noise deteriorates the signal to noise ratio. As a result, the temperature distribution on the chip surface fluctuates more obviously than that at 1980 fps, indicating worse uniformity.

In Fig. 5 and Fig. 6, average transient temperature distribution from a  $25 \times 30$  pixels box is extracted to compare with that by the TI method. Same as Case I, the heating and cooling process exhibit much faster time response by h-SCRLI method at 5600 fps ( $179 \mu\text{s}$ ), 200 times faster than that by TI. The rising and falling time correspond to 150 ms and 110 ms at 5600 fps driven under 500 mA, respectively. The high speed camera reaches the maximum frame rate at 14600 fps, corresponding to  $68 \mu\text{s}$  in time resolution, with sacrifice of picture size of  $144 \times 128$  pixels in this case.

Fig. 7 demonstrates spatial resolution comparison between the proposed h-SCRLI and the TI method. As the same operation in Fig. 4, a horizontal line labeled as L02 is drawn horizontally along chip surface, as displayed in Fig. 7(a) and (b). Similarly, the horizontal temperature distribution by h-SCRLI exhibits much better spatial resolution and sensitivity than that by TI, as shown in Fig. 7(c).

## V. CONCLUSION

In this work, we propose a reflected light-based non-contact method to detect the transient two-dimensional temperature

distribution of LED chip by high-speed camera. Comparing with the conventional infrared thermal imaging, the spatial resolution of the proposed method is only limited to that of optical microscope, i.e., submicron scale in this system, the time resolution of the proposed method is up to  $505 \mu\text{s}$  at 1980 fps,  $179 \mu\text{s}$  at 5600 fps, and  $68 \mu\text{s}$  at 14600 fps of the maximum frame rate of the high-speed camera, respectively. At high frame rates, less exposure time results in much more noise which in turn deteriorates the uniformity of 2D temperature distribution. Further measures shall be adopted to improve the signal to noise ratio.

## REFERENCES

- [1] N. Grossman *et al.*, "Multi-site optical excitation using ChR2 and micro-LED array," *J. Neural Eng.*, vol. 7, no. 1, Feb. 2010, Art. no. 16004.
- [2] H.-L. Ke *et al.*, "Analysis of junction temperature and modification of luminous flux degradation for white LEDs in a thermal accelerated reliability test," *Appl. Opt.*, vol. 55, no. 22, pp. 5909–5916, Aug. 2016.
- [3] L. Trevisanello *et al.*, "Accelerated life test of high brightness light emitting diodes," *IEEE Trans. Device Mater. Rel.*, vol. 8, no. 2, pp. 304–311, Jun. 2008.
- [4] K. Maize, J. Christofferson, and A. Shakouri, "Transient thermal imaging using thermoreflectance," in *Proc. IEEE Semicond. Thermal Meas. Manage. Symp.*, San Jose, CA, USA, Apr. 2008, pp. 55–58.
- [5] Y. Xi and E. F. Schubert, "Junction-temperature measurement in GaN ultraviolet light-emitting diodes using diode forward voltage method," *Appl. Phys. Lett.*, vol. 85, no. 12, pp. 2163–2165, Sep. 2004.
- [6] H. Youl, K. H. Ha, and J. H. Chae, "Measurement of junction temperature in GaN-based laser diodes using voltage-temperature characteristics," *Appl. Phys. Lett.*, vol. 87, no. 9, pp. 1–3, Aug. 2005.
- [7] J. Jin *et al.*, "A microscopic hyperspectral-based centroid wavelength method for measuring two-dimensional junction temperature distribution of LEDs," *IEEE Electron Device Lett.*, vol. 40, no. 4, pp. 506–509, Apr. 2019.
- [8] J. Zhang, Z. Tao, S. Liu, S. Yuan, Y. Jin, and S. Yang, "Feasibility analysis of junction temperature measurement for GaN-based high-power white LEDs by the peak-shift method," *Chin. Opt. Lett.*, vol. 11, no. 9, pp. 44–48, Sep. 2013.
- [9] C. J. Hayes, K. B. Walsh, C. V. Greensill, "Light-emitting diodes as light sources for spectroscopy: Sensitivity to temperature," *J. Near Infrared Spectrosc.*, vol. 25, no. 6, pp. 416–422, Oct. 2017.
- [10] Y. Lin *et al.*, "Determining phosphor temperature in light-emitting diode based on divisional normalized emission power," *IEEE Electron Device Lett.*, vol. 40, no. 10, pp. 1650–1653, Oct. 2019.
- [11] Y. Gu and N. Narendran, "A non-contact method for determining junction temperature of phosphor-converted white LEDs," in *Proc. SPIE*, vol. 5187, Jan. 2004, pp. 107–114.
- [12] E. Tamdogan, G. Pavlidis, M. Arik, and S. Graham, "A comparative study on the junction temperature measurements of LEDs with Raman spectroscopy, microinfrared (IR) Imaging, and forward voltage methods," *IEEE Trans. Compon. Packag. Technol.*, vol. 8, no. 11, pp. 1914–1922, Nov. 2018.
- [13] T. Park, Y.-J. Guan, Z.-Q. Liu, and Y. Zhang, "In operando micro-Raman three-dimensional thermometry with diffraction-limit spatial resolution for GaN-based light-emitting diodes," *Phys. Rev. Appl.*, vol. 10, no. 3, Sep. 2018, Art. no. 034049.
- [14] Y. P. Ma, R. Hu, X. J. Yu, W. C. Shu, and X. B. Luo, "A modified bidirectional thermal resistance model for junction and phosphor temperature estimation in phosphor-converted light-emitting diodes," *Int. J. Heat Mass Transf.*, vol. 106, pp. 1–6, Mar. 2017.
- [15] J. Fan, W. Chen, and W. Yuan, "Dynamic prediction of optical and chromatic performances for light-emitting diode array based on a thermal-electrical-spectral model," *Opt. Exp.*, vol. 28, no. 9, pp. 13921–13937, 2020.
- [16] Y. Gao *et al.*, "Two-dimensional temperature distribution measurement of light-emitting diodes by micro-hyperspectral imaging-based reflected light method," *Opt. Exp.*, vol. 27, no. 6, pp. 7945–7954, Mar. 2019.